

Crystal Packing: An Examination of the Packing of Molecules Approximately Isosteric with 4,5-Dichlorophthalic Anhydride

by Doyle Britton*, Wayland E. Noland, Matthew J. Pinnow, and Victor G. Young Jr.

Department of Chemistry, University of Minnesota, Minneapolis, Minnesota 55455-0431
(phone: 612-625-9535; fax: 612-626-7541; e-mail: britton@chem.umn.edu)

Dedicated to Professor *Jack D. Dunitz* on the occasion of his 80th birthday

The crystal structures of five 5,6-disubstituted benzofurazan 1-oxides are presented and compared with five previously reported structures: three polymorphs of 5,6-dichlorobenzofurazan 1-oxide plus 4,5-dichloro- and 4,5-dibromophthalic anhydride. All but one of these compounds pack with similar two-dimensional layers. The benzofurazan oxides all show disorder about a crystallographic twofold or pseudo-twofold axis. In addition, six complexes of phthalic anhydride and benzofurazan oxides are reported. With the packing in the complexes principally directed by the π complexing, the disorder, invariably found in the uncomplexed benzofurazan oxides, is diminished, and, in two cases, eliminated.

Introduction. – Recently, the crystal structures of 4,5-dichlorophthalic anhydride (**Cl2PA**), 4,5-dibromophthalic anhydride (**Br2PA**), and 4,5-dichlorobenzofurazan 1-oxide (**Cl2BF**) were reported by *Ojala et al.* [1]. The original purpose was to explore the crystallographic isostructuralism of **Cl2PA** and **Cl2BF** [2], an isostructuralism that requires disordered **Cl2BF** to mimic the shape of **Cl2PA**. (see *Fig. 1* for the original compounds plus the related compounds to be reported here). In the course of the original work, three polymorphs were found for **Cl2BF**, and a partial isostructural relationship was found between **Cl2PA**, which is isostructural with one of the polymorphs of **Cl2BF**, and **Br2PA**.

A summary of the results follows. The molecules in all five structures align in ribbons along twofold or pseudo-twofold axes. These ribbons appear to be held together by *Lewis* acid–base interactions between Cl or Br, and O. In four of the five structures, **Cl2PA**, **Br2PA**, **Cl2BF-A**, and **Cl2BF-C**, these ribbons align side-to-side to form roughly planar sheets (in the fifth structure, **Cl2BF-B**, the sheet is significantly puckered). The sheets appear to be held together by C–H \cdots O and C–H \cdots N interactions. A sheet of **Cl2PA** is shown in *Fig. 2*. In **Cl2BF-A**, the **Cl2BF** molecules are disordered about the twofold axis to mimic **Cl2PA** molecules. The sheets stack together in similar ways in **Cl2PA**, **Br2PA**, and **Cl2BF-A**, but in a distinctly different fashion in **Cl2BF-C**. The similarity in the packing between **Cl2PA** and **Br2PA** is quite close even though the space group is *C2/c* for **Cl2PA** while it is *C-1* for **Br2PA**.

This work is extended here (see *Fig. 1*). First, **Br2BF** is included, which completes the previous comparison. Then, **BrClBF**, **BrMeBF**, and **IMeBF** are examined to see whether removing the equivalence between the X and Y substituents would reduce or eliminate the disorder in the packing. These were chosen since Cl, Br, I, and Me all have different *Lewis* acid strengths, Br > Cl, and Br and I > Me. In every case, one might be

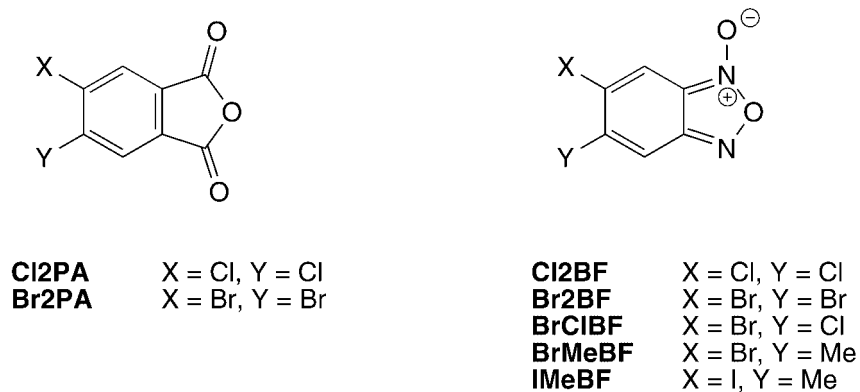


Fig. 1. The **PA** and **BF** molecules referred to in this work. The abbreviations given are those used throughout the paper. When it is necessary to distinguish between the two isomers, **XYBF** will refer to the isomer with X in the 6-position, *i.e.*, closest to the exocyclic O-atom, and **YXBF** to the isomer with X in the 5-position.

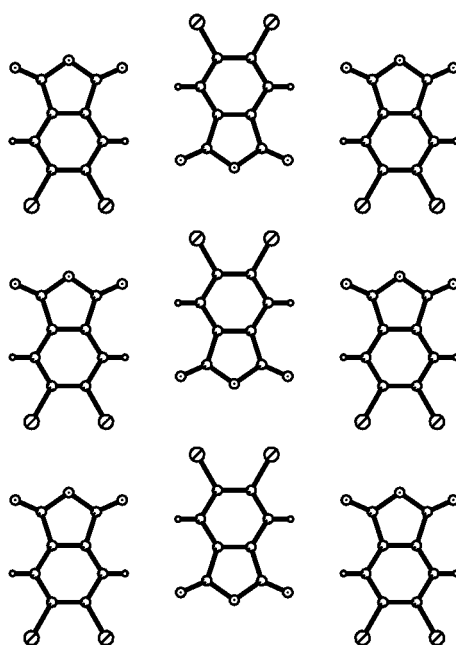


Fig. 2. A layer in the structure of **Cl₂PA**. A layer in **Br₂PA** is quite similar, although the two repeat directions in the latter differ slightly from orthogonal. Layers in **Cl₂BF-A** and **Cl₂BF-C** are similar except for disorder about the twofold axes.

expected to be favored over the other and lead to less disorder, or, indeed, lead to ordered or completely different structures. Finally, when it was found that the disorder was not completely eliminated, pyrene complexes of all of the compounds (except **BrClBF**) were examined. The latter extension of the work was based on the idea that it

might be possible to use π complexes to facilitate σ interactions between the benzofurazan (**BF**) or phthalic anhydride (**PA**) molecules. This use of π complexes can be seen, for example, in *Desiraju* and co-workers [3], or *Britton* [4].

For an introduction to the history and noncrystallographic properties of benzofurazan 1-oxides, see *Katritzky* and *Gordeev* [5].

Crystallographic Results. – Crystallographic data are given in *Table 1*. All of the bond lengths and angles are normal within experimental error. The anisotropic displacement parameters are reasonable. As an example, a drawing of the anisotropic displacement ellipsoids in **BrMeBF** is given in *Fig. 3*; the rest are similar. As a summary of the displacement parameters, the ranges of the equivalent isotropic displacement parameters are given for all of the **PA** and **BF** molecules in *Table 2*. Also shown in *Fig. 3* are the disordered molecules of **BrMeBF**; again, the other compounds are similar.

All of the uncomplexed molecules in this study and the previous one, except **C12BF-B**, form two-dimensional sheets that are isostructural with each other (see *Fig. 2*), although they are not all isostructural in three dimensions. There are four different stacking patterns of the layers. These are shown in *Fig. 4*. The unit cells given in *Table 1* are the conventional cells. In *Table 3*, the unit cells for the uncomplexed molecules are converted to new cells in which a' is the repeat distance parallel to the ribbon direction, b' is the repeat distance closest to perpendicular to a' in the plane of the layer, and c' is the repeat distance closest to normal to the $a'b'$ plane. The constancy of the a' values and of the b' values (except for **C12BF-B**, which has puckered sheets), and the close match of γ' to 90° demonstrates the similarity of the layers. The variations in the values of c' , α' , and β' testify to the differences in the stacking of the layers.

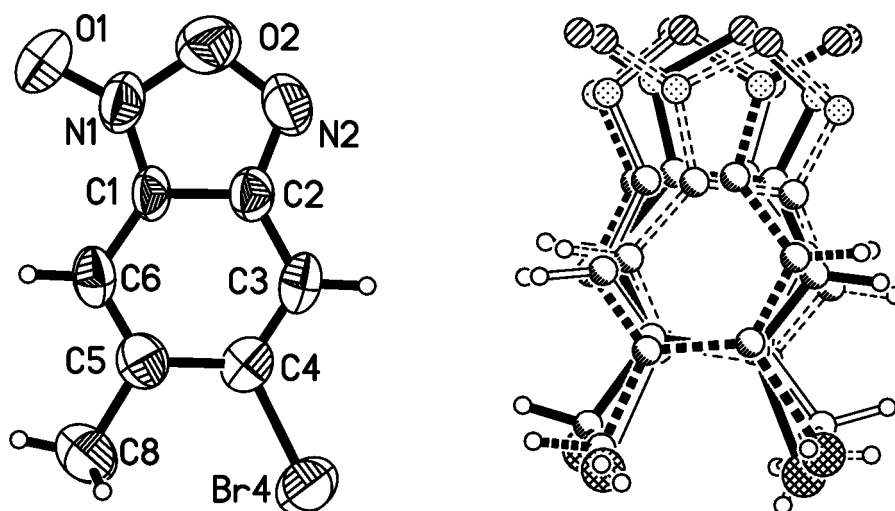


Fig. 3. Left: Anisotropic displacement ellipsoids (50% probability) for **BrMeBF**. The atom labelling shown is used throughout. Right: The four disordered orientations: solid bonds: 0.483 occupancy; solid dashed: 0.217; open: 0.209; open dashed: 0.091.

Table 1. Crystal Data and Structure-Refinement Details

	Br2BF-A	BrClBF-A	BrClBF-C	BrMeBF	IMeBF	Cl2PA/py	Cl2BF/py	Br2BF/py	Br2PA/py	BrMeBF/py	IMeBF/py
Empirical formula	C ₆ H ₂ Br ₂ N ₂ O ₂ ·A	C ₆ H ₂ BrClN ₂ O ₂ ·A	C ₆ H ₂ BrClN ₂ O ₂ ·C	C ₇ H ₃ BrN ₂ O ₂	C ₇ H ₃ IN ₂ O ₂	C ₈ H ₂ Cl ₂ O ₃ ·C ₁₆ H ₁₀	C ₆ H ₂ Cl ₂ N ₂ O ₂ ·C ₁₆ H ₁₀	C ₆ H ₂ Br ₂ N ₂ O ₂ ·C ₁₆ H ₁₀	C ₈ H ₂ Br ₂ O ₃ ·C ₁₆ H ₁₀	C ₇ H ₃ BrN ₂ O ₂ ·1.5(C ₁₆ H ₁₀)	C ₇ H ₃ IN ₂ O ₂ ·C ₁₆ H ₁₀
Crystal system	monoclinic	monoclinic	monoclinic	triclinic	triclinic	monoclinic	monoclinic	monoclinic	monoclinic	triclinic	monoclinic
Space group	<i>C2/c</i>	<i>C2/c</i>	<i>C2/c</i>	<i>P1</i>	<i>P1</i>	<i>P2₁/n</i>	<i>P2₁/n</i>	<i>P2₁/n</i>	<i>P2₁/n</i>	<i>P1</i>	<i>P2₁/c</i>
<i>a</i> /Å	11.687(3)	11.545(3)	7.2868(18)	6.1809(15)	6.3381(16)	6.2985(17)	6.7858(17)	6.8334(17)	13.516(4)	7.3295(18)	14.955(4)
<i>b</i> /Å	9.087(2)	9.010(2)	9.150(2)	8.041(2)	8.510(2)	16.236(4)	15.487(4)	15.809(4)	9.669(2)	8.550(2)	17.564(4)
<i>c</i> /Å	7.4165(19)	7.3350(18)	11.757(3)	9.295(2)	9.605(2)	17.096(4)	17.092(4)	17.147(4)	14.451(4)	19.185(5)	14.329(4)
<i>α</i> /°				67.470(10)	63.770(10)					88.150(10)	
<i>β</i> /°	96.050(10)	95.830(10)	96.210(10)	74.430(10)	71.940(10)	96.370(10)	91.260(10)	90.580(10)	99.000(10)	79.180(10)	95.930(10)
<i>γ</i> /°				77.909(010)	74.130(10)					87.080(10)	
<i>V</i> /Å ³	783.2(4)	7.59.0(3)	779.3(3)	407.3(2)	436.1(2)	1884.0(8)	1795.8(8)	1852.3(8)	1865.3(9)	1179.0(5)	3743.7(17)
<i>Z</i>	4	4	4	2	2	4	4	4	4	2	8
<i>D</i> _{calc} /g cm ⁻³	2.492	2.183	2.126	1.868	2.102	1.478	1.506	1.779	1.810	1.500	1.697
<i>F</i> (000)	552	480	480	224	260	856	832	976	1000	542	1888
Crystal size/mm	0.50 × 0.15 × 0.05	0.50 × 0.15 × 0.15	0.20 × 0.20 × 0.05	0.50 × 0.30 × 0.08	0.50 × 0.38 × 0.22	0.50 × 0.32 × 0.26	0.45 × 0.15 × 0.10	0.40 × 0.05 × 0.05	0.45 × 0.40 × 0.20	0.40 × 0.20 × 0.10	0.40 × 0.12 × 0.08
<i>μ</i> /mm ⁻¹	10.30	5.72	5.57	5.00	3.631	0.369	0.383	4.398	4.371	1.777	1.733
Temp./K	174(2)	174(2)	174(2)	297(2)	297(2)	174(2)	174(2)	173(2)	173(2)	174(2)	174(2)
Wavelength/Å	0.71073	0.71073	0.71073	0.71073	0.71073	0.71073	0.71073	0.71073	0.71073	0.71073	0.71073
<i>θ</i> Range/°	2.85–27.49	2.87–25.03	3.49–25.01	2.42–25.00	2.42–25.08	1.73–24.95	1.77–25.11	1.75–27.55	1.92–25.19	2.16–27.54	1.37–27.49
<i>hkl</i> Range	–15 < <i>h</i> < 15 –11 < <i>k</i> < 11 –9 < <i>l</i> < 9	–9 < <i>h</i> < 13 –10 < <i>k</i> < 10 –8 < <i>l</i> < 8	–8 < <i>h</i> < 8 –9 < <i>k</i> < 10 –13 < <i>l</i> < 13	–7 < <i>h</i> < 7 –9 < <i>k</i> < 9 –11 < <i>l</i> < 10	–7 < <i>h</i> < 7 –10 < <i>k</i> < 9 –11 < <i>l</i> < 10	–7 < <i>h</i> < 8 –17 < <i>k</i> < 19 –17 < <i>l</i> < 20	–8 < <i>h</i> < 8 –12 < <i>k</i> < 18 –19 < <i>l</i> < 20	–8 < <i>h</i> < 8 –20 < <i>k</i> < 20 –22 < <i>l</i> < 22	–16 < <i>h</i> < 15 –11 < <i>k</i> < 11 –17 < <i>l</i> < 17	–9 < <i>h</i> < 9 –11 < <i>k</i> < 11 –24 < <i>l</i> < 24	–19 < <i>h</i> < 19 –22 < <i>k</i> < 22 –18 < <i>l</i> < 18
Reflections: collected, unique, observed (<i>I</i> > 2σ(<i>I</i>))	3945, 901, 804	1883, 669, 635	1913, 678, 552	2789, 1418, 1061	2870, 1522, 1154	9055, 3249, 2326	8742, 3145, 2400	20772, 4249, 2565	21571, 3438, 1957	13745, 5327, 2776	37559, 8548, 6001
Number of parameters, constraints	103, 60	117, 69	122, 69	227, 190	227, 361	320, 35	253	253	263	443, 213	555, 90
<i>R</i> (<i>F</i>)	0.033	0.036	0.037	0.044	0.041	0.041	0.041	0.052	0.052	0.059	0.038
<i>wR</i> (<i>F</i> ²) all data	0.086	0.095	0.102	0.128	0.127	0.111	0.111	0.104	0.107	0.144	0.095
Goodness-of-fit	1.05	1.04	1.09	1.05	0.94	0.95	1.00	0.97	0.90	1.01	1.02
max/min resid.	0.72, –0.75	0.60, –0.60	0.47, –0.43	0.26, –0.35	0.29, –0.28	0.18, –0.22	0.27, –0.27	0.53, –0.42	0.96, –0.66	0.36, –0.29	1.62, –0.45
dens./e Å ³											
CCDC No.	200604	200695	200696	200920	200921	201419	201417	201418	201420	201534	201421

^a) Crystallographic data (excluding structure factors) have been deposited with the Cambridge Crystallographic Data Centre (CCDC). Deposition Nos. are given in the Table. Copies of the data can be obtained, free of charge, on application to the CCDC, 12 Union Road, Cambridge CB2 1EZ, UK (fax: +44(1223)336033; e-mail deposit@ccdc.cam.ac.uk.).

Table 2. Ranges of Equivalent Isotropic Thermal Parameters for All of the **PA** and **BF** Molecules

Molecule	T/K	Range U_{eq}	Molecule	T/K	Range U_{eq}
Cl2PA	297	0.038–0.065	Cl2PA/py	174	0.033–0.064
Br2PA	297	0.036–0.061	Br2PA/py	173	0.029–0.051
Cl2BF-A	173	0.020–0.034	Cl2BF/py	174	0.038–0.055
Cl2BF-C	173	0.028–0.051			
Br2BF-A	174	0.024–0.042	Br2BF/py	173	0.029–0.061
BrClBF-A	174	0.020–0.032			
BrClBF-C	174	0.034–0.056			
BrMeBF	297	0.044–0.096	BrMeBF/py	174	0.032–0.055
IMeBF	297	0.075–0.112	IMeBF/py	174	0.030–0.053

Table 3. Cell Constants Based on Similar Layers in the Uncomplexed Compounds. The first five entries are taken from [1].

Compound	a'	b'	c'	α'	β'	γ'	Space group	Matrix
Cl2PA	8.994	13.775	7.423	119.65	90	90	$I2/a$	a)
Br2PA	9.209	13.917	7.628	113.56	105.08	89.89	$C-1$	b)
Cl2BF-A	8.871	12.937	7.222	118.66	90	90	$I2/a$	a)
Cl2BF-B	9.011	11.750	7.068	90	98.56	90	$P2_1/n^c$	d)
Cl2BF-C	9.055	13.059	7.223	118.10	90	90	$I2/a$	e)
Br2BF-A	9.087	13.165	7.417	118.02	90	90	$I2/a$	a)
BrClBF-A	9.010	13.034	7.335	118.22	90	90	$I2/a$	a)
BrClBF-C	9.150	13.145	7.287	117.23	90	90	$I2/a$	e)
BrMeBF	9.243	13.066	7.889	114.20	112.08	91.04	$C-1$	f)
IMeBF	9.605	13.195	8.509	112.47	116.23	90.74	$C-1$	f)

a) 0,1,0/1,0,1/0,0, – 1. b) 0,1,0/ – 1,0, – 1/0,0, – 1. c) This is $(P2_1/n11)$. d) 0,0,1/0,1,0/ – 1,0,0. e) 0, – 1,0/1,0,1/ – 1,0,0. f) 0,0,1/ – 2,1,0/0, – 1,0.

The complexes with pyrene show more variety. **Cl2BF/py**, and **Br2BF/py** are isostructural, at least to the extent of similar cell constants and packing; there is a significant difference in the amount of disorder. **Cl2PA/py** has cell constants similar to the previous two, but there is a difference in the packing. **Br2PA/py** and **IMeBF/py** are different from each other, and from the previous three complexes. **BrMeBF/py** is distinctly different; the **BrMeBF/py** ratio is 2:3 rather than the 1:1 found in the other five. Owing to the limited supply of **BrMeBF** available, it was not possible to repeat the preparation with different proportions of the two compounds, although this is worth doing. It would also be of interest to see if other 2:3 complexes could be formed.

In all of the complexes with pyrene the **PA** and **BF** molecules are in stacks in which they alternate with pyrene molecules in the familiar mode for π complexes. These stacks are packed in hexagonal arrays except in the **BrMeBF/py** where the ratio of molecules is 2:3. In this case, double layers of stacks are separated by layers of pyrene that lie parallel to the stack direction.

Since our interest in this paper is in the σ interactions between **BF** or **PA** molecules, only these molecules are shown in the packing diagrams. In all of the packing diagrams, only the predominant orientation of the disorder is shown. In all of the packing diagrams (Figs. 5–9 below), the pyrene (not shown) is stacked directly above and

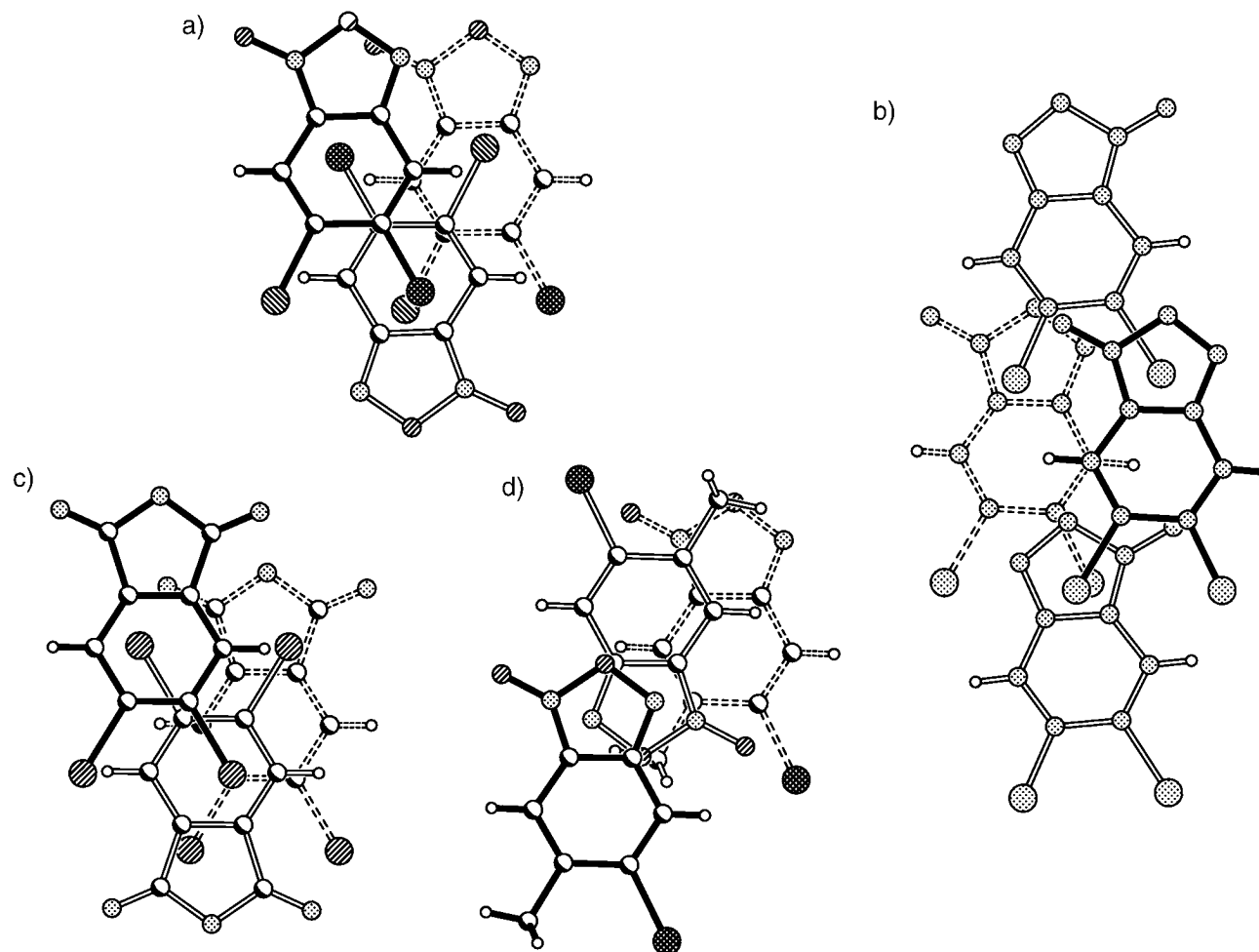


Fig. 4. The stacking of the layers in the various structural types, drawn normal to the plane of the uppermost molecule. The orientation with the highest occupancy has been shown in each case (see Table 5). The solid bonds show the top, the open bonds the next, and the dotted bonds the bottom layer. *a*) Stacking in **BrCIBF-A** (shown), **Cl2PA**, **Cl2BF-A**, **Br2BF-A**. *b*) **BrCIBF-C** (shown), **Cl2BF-C**. *c*) **Br2PA**. *d*) **BrMeBF** (shown), **IMeBF**.

below the **PA** or **BF** molecules. The metric data for the $X \cdots Y$ ($X = \text{Cl, Br, or Me}$; $Y = \text{O or N}$) interactions are given in *Table 4*.

Table 4. *Metric Parameters for the Intermolecular $A \cdots B$ Interactions in the Approximate Plane of the Molecule*

Compound	A	B	$C-A \cdots B/^\circ$	$A \cdots B/\text{\AA}$	$A \cdots B-(\text{or N})/^\circ$
Cl2PA	Cl(4)	O(3)	161	3.33	103
	Cl(4)	O(2)	122	3.33	97
	Cl(5)	O(2)	122	3.33	97
Br2PA	Cl(5)	O(1)	161	3.33	103
	Br(4)	O(3)	156	3.43	105
	Br(4)	O(2)	119	3.49	96
Cl2BF-A	Br(5)	O(2)	121	3.44	96
	Br(5)	O(1)	159	3.40	104
	Cl(4)	O(2)	131	3.09	107
Cl2BF-C	Cl(5)	O(2)	118	3.59	89
	Cl(5)	O(1)	156	3.19	114
	Cl(4)	O(2)	134	3.19	108
Br2BF	Cl(5)	O(2)	117	3.83	89
	Cl(5)	O(1)	154	3.36	117
	Br(4)	O(2)	131	3.18	106
BrClBF-A	Br(5)	O(2)	113	3.73	88
	Br(5)	O(1)	151	3.29	115
	Cl(4)	O(2)	131	3.26	106
BrClBF-C	Br(5)	O(2)	115	3.63	89
	Br(5)	O(1)	153	3.24	113
	Cl(4)	O(2)	135	3.32	110
BrMeBF	Br(5)	O(2)	114	3.83	88
	Br(5)	O(1)	151	3.35	116
	Br(4)	O(2)	138	3.27	112
IMeBF	H(8B)	O(2)	122	3.69	90
	H(8B)	O(1)	119	3.29	114
	H(6)	O(1)	123	2.68	123
Cl2PA/py	I(4)	O(2)	142	3.38	118
	H(8B)	O(2)	124	4.23	85
	H(8B)	O(1)	123	3.58	123
Br2PA/py	Cl(5)	O(1)	128	3.28	131
	Br(5)	O(1)	163	3.39	122
Cl2BF/py	Br(4)	O(1)	127	3.63	136
	Cl(5)	O(1)	144	3.26	111
Br2BF/py	Cl(5)	O(2)	125	3.76	83
	Br(5)	O(1)	146	3.24	110
BrMeBF/py	Br(5)	O(2)	126	3.73	82
	Br(5)	O(1)	141	3.30	101
IMeBF/py^{a)}	Br(5)	O(2)	109	3.59	85
	H(7A)	O(2)	156	2.74	140
	I(5)a	N(2)a	175	3.12	136
	I(5)b	N(2)b	173	3.38	128
	H(6)a	O(1)b	139	2.84	127
	H(6)b	O(1)a	144	2.84	134
	H(7C)a	O(2)b	147	3.43	110
	H(7A)b	O(2)a	149	3.31	110

^{a)} There are two crystallographically independent molecules, a and b.

A layer of **C12BF** in **C12BF/py** is shown in *Fig. 5*. The molecules form puckered ribbons parallel to the *b* axis. The packing in **Br2BF/py** is the same except that there is disorder with **C12BF** and none with **Br2BF**.

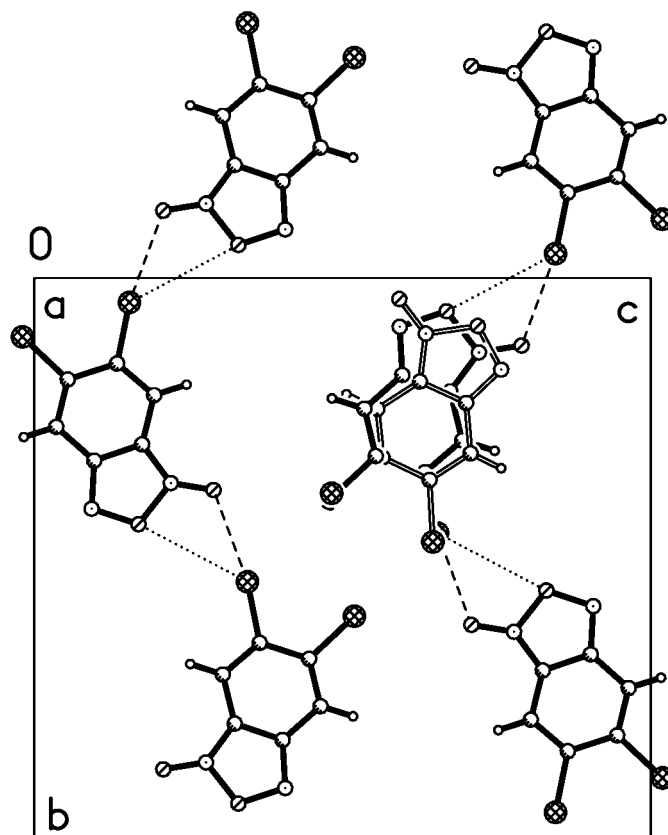


Fig. 5. Packing of **C12BF** in the complex with pyrene. The predominant orientation is shown with solid bonds. The other orientation is shown with open bonds. The short Cl...O contact is shown with dashed lines. In the **Br2BF/py** complex, the arrangement is the same except there is no disorder.

A layer of **C12PA** in **C12PA/py** is shown in *Fig. 6*. The molecules form parallel ribbons similar to those in **C12BF/py**, but a comparison of the two packings shows that the sideways tilts of the molecules in the ribbons are in the opposite sense in the two cases. Additionally, the disorder in the **C12PA** is end-for-end rather than side-to-side as it is in **C12BF/py**. This is the only example of end-for-end disorder that was found.

A layer of **Br2PA** in **Br2PA/py** is shown in *Fig. 7*. This is a double ribbon parallel to both the (001) plane and the *c* axis. The contacts perpendicular to the ribbon direction (dashed lines) are shorter (stronger) than those parallel to it (dotted lines).

A layer of **BrMeBF** in **BrMeBF/py** is shown in *Fig. 8*. There are double ribbons of molecules parallel to the *b* direction. These double ribbons are far from flat, but can be viewed as the beginning of a sheet similar to those found in the uncomplexed compounds (see *Fig. 2*).

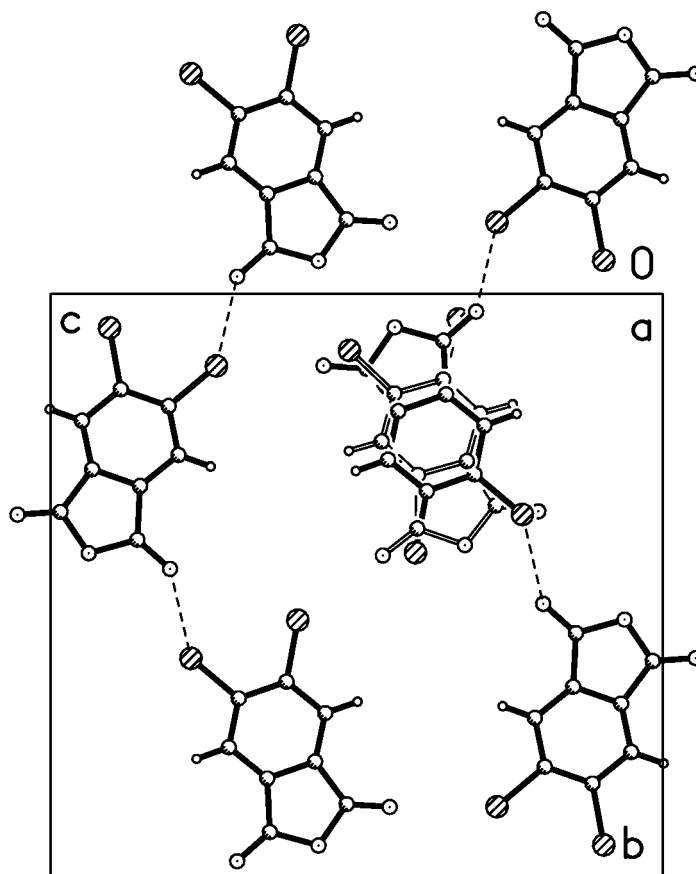


Fig. 6. Packing of **Cl₂PA** in the complex with pyrene. Same conventions as in Fig. 5. Note that the arrangement of the molecules along the chains is not the same as in Fig. 5.

A layer of **IMeBF** in **IMeBF/py** is shown in Fig. 9. There are two crystallographically independent, but similar, ribbons parallel to the *b* axis. Each ribbon is held together by I⋯N interactions. There are also ring H⋯O interactions between adjacent ribbons. The two ribbons differ in that the ribbon near $a = 1/2$ is ordered, while the ribbon near $a = 0$ is disordered, as shown. The two independent molecules are related to each other through pseudo-symmetry. For example, the two molecules in the lower left-hand corner of Fig. 9 are related by a pseudo-inversion center near $3/4, 1/8, 3/4$.

Disorder was prevalent in the **PA** and **BF** molecules, both uncomplexed and in the complexes with pyrene (see Fig. 3 for an example). The occupancies of the various disordered arrangements are given in Table 5. In the **XYBF** compounds, the disorder includes both disorder about a twofold or pseudo-twofold axis, and disorder due to the presence of the two isomers **XYBF** and **YXBF**.

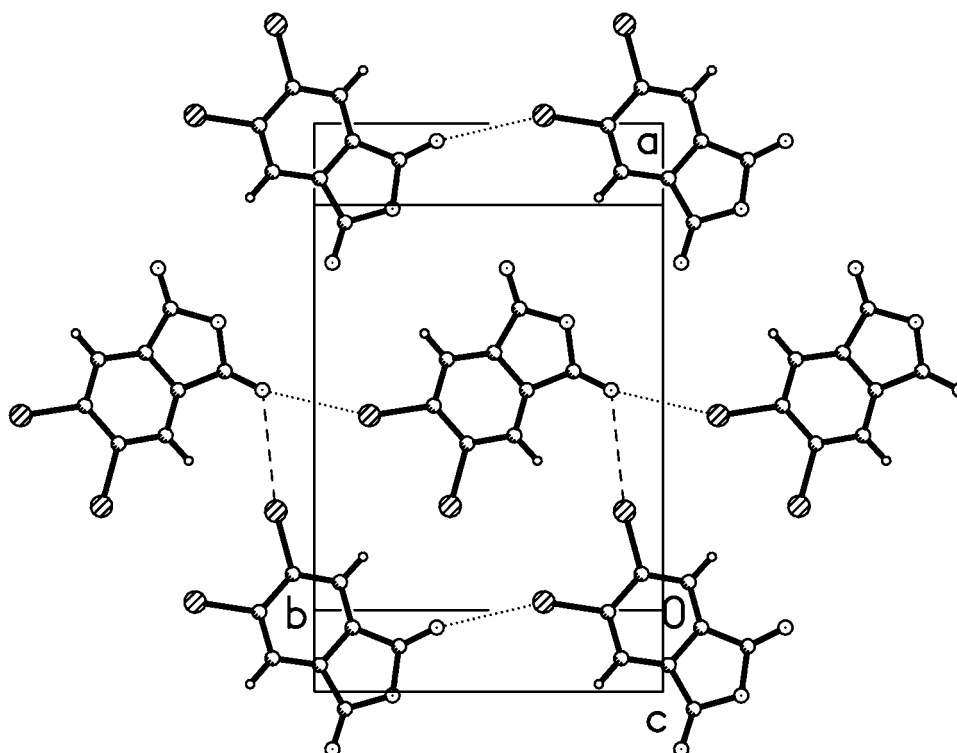


Fig. 7. Packing of **Br₂PA** in the complex with pyrene. The shorter (stronger) Br...O distances are shown as dashed lines; the longer as dotted lines.

Discussion. – *Phthalic Anhydride Structures.* The **PA** compounds and complexes were intended to serve as reference structures. No disorder was anticipated, but in **Cl₂PA/py** (Fig. 6) there is end-for-end disorder that is not present in any of the other structures. In the uncomplexed structures, which are isostructural, both halogen atoms are in contact with two O-atoms each, for a total of four X...O contacts (Fig. 2 and Table 4). In the complexed structures, the two **PA** complexes are no longer isostructural. In the **Cl₂PA/py**, there is only one Cl...O contact, at about the same distance as in **Cl₂PA**. In the **Br₂BF/py**, there is one Br...O contact at about the same distance as in **Br₂PA**, and a second, put in for comparison only, at a longer distance than a normal *Van der Waals* contact.

The Uncomplexed Structures. In **Cl₂BF-A** and **-C**, and **Br₂BF-A**, the disorder is across a crystallographic two fold axis, so the disorder must be 50:50. In **BrCIBF-A**, there is also close to complete disorder between the two isomers, **BrCIBF** and **ClBrBF**. In **BrCIBF-C**, the disorder is even closer to complete; there is no significant difference among any of the four possible orientations or isomers (Table 5). The replacement of two Cl or two Br by one Cl and one Br has no significant effect on the ordering.

That **BrCIBF-C** is slightly more disordered is consistent with the larger *a'* and *b'* dimensions (see Table 3). The looser packing is also consistent with the larger

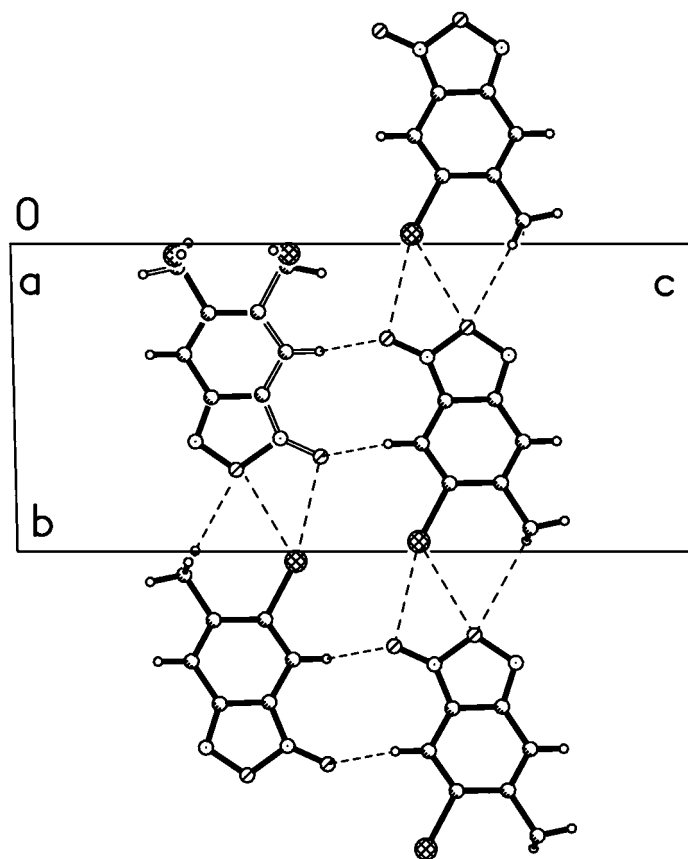


Fig. 8. Packing of **BrMeBF** in the complex with pyrene. Contacts between O-atoms, and Me H- and Br-atoms are shown as dashed lines.

displacement parameters (see *Table 2*). *Dunitz* [6] has pointed out that the most closely packed polymorph should be the low-temperature form. The melting-point behavior (see *Crystallography: Experimental*) is consistent with this; A is the low and C the high-temperature form.

In **BrMeBF** and **IMeBF**, the occupancies are far from equal. In both cases, the **MeXBF** isomer is more-abundant than the **XMeBF** isomer, and one of the two orientations of the **MeXBF** is more abundant than the other. It is surprising that the Me groups, which replace halogen atoms while leaving the structure otherwise isostructural with all the other **BF** compounds, do not have any short contacts to the O-atoms. The H \cdots O distances (*Table 4*) are much larger than the usual C–H \cdots O *Van der Waals* distances.

The change from **BrClBF** to **BrMeBF** might be expected to have a greater effect on the packing than the change from **Cl2BF** to **BrClBF**. It did, but only to the extent of favoring one isomer over the other in the same disordered arrangement. Likewise, the change from **BrMeBF** to **IMeBF** might also be expected to have an effect on the

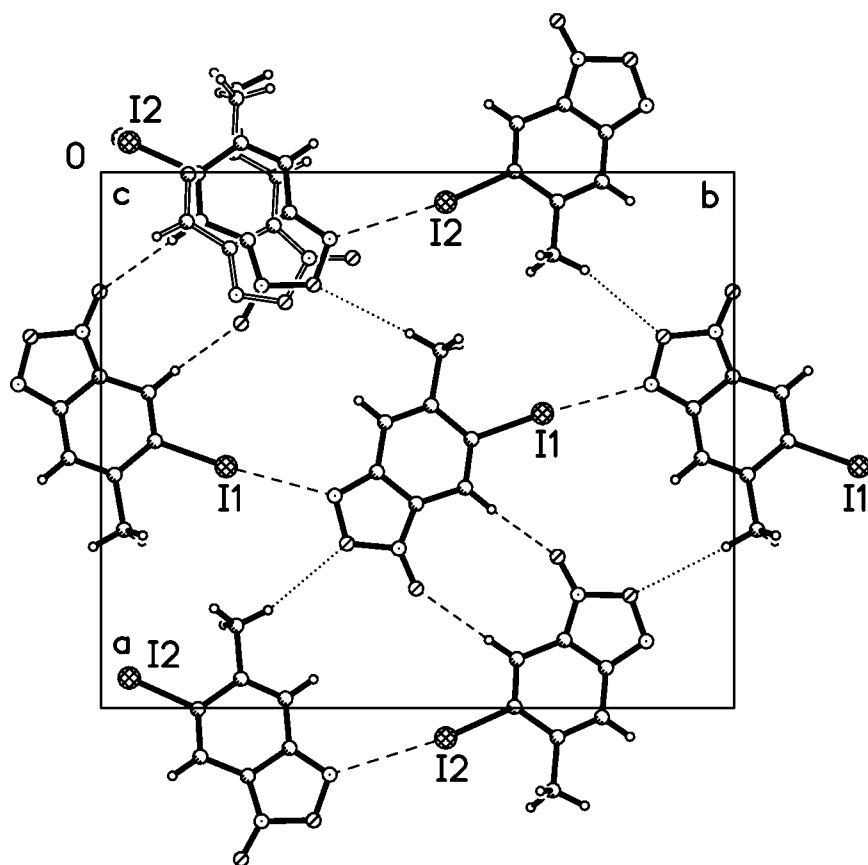


Fig. 9. Packing of **IMeBF** in the complex with pyrene. The rows along $a \sim 0$ and 1 are crystallographically independent from the row at $a \sim 1/2$. $I \cdots N$ and ring $H \cdots O$ interactions are shown with dashed lines. The weaker $CH_3 \cdots O$ interactions are shown with dotted lines.

packing, but it did not. The general arrangement is the same, and the distribution of occupancies is not greatly different between the two.

The Pyrene Complexes. In four of the six complexes, the molecular volume is larger than the sum of the molecular volumes of the pyrene plus the **PA** or **BF**; only in the **Br2PA** and **IMeBF** complexes is the packing more efficient for the complex than for the separated structures. There is very little disorder in the two efficiently packed complexes, but even in the more loosely packed complexes there is considerably less disorder than in the uncomplexed compounds (see *Table 5*). The result found, decreased disorder in the complexes, is what was looked for, but it is still surprising.

In the **Cl2BF/py** crystal, one orientation of the **Cl2BF** is strongly favored over the other. In the isostructural **Br2BF/py**, the same preferred orientation is found in an ordered crystal. In each case there is only one significant $X \cdots O$ contact, although a second distance is given for comparison (*Table 4*). The short distances are slightly longer than in the uncomplexed structures.

Table 5. Degree of Disorder in the Phthalic Anhydride and Benzofurazan 1-Oxide Molecules

Compound	Orientation in the plane of the molecule ^{a)}			
	ONON XY	NONO YX	ONON YX	NONO XY
Cl2PA	ordered			
Br2PA	ordered			
Cl2BF-A	0.5	0.5	–	–
Cl2BF-B^{a)}	0.622(4)	0.378(4)	–	–
Cl2BF-C	0.5	0.5	–	–
Br2BF	0.5	0.5	–	–
BrClBF-A	0.282(9)	0.282(9)	0.218(9)	0.218(9)
BrClBF-C	0.254(11)	0.254(11)	0.246(11)	0.246(11)
BrMeBF^{a)}	0.091(4)	0.209(4)	0.483(4)	0.217(4)
IMeBF^{a)}	0.119(4)	0.105(3)	0.435(3)	0.341(4)
Cl2PA/py	end-for-end disorder 0.716(2)/0.284(2)			
Br2PA/py	ordered			
Cl2BF/py^{a)}	0.822(3)	0.178(3) around a pseudo-twofold axis		
Br2BF/py	ordered			
BrMeBF/py^{a)}	0.510(5)	0.056(4)	0.311(4)	0.123(5)
IMeBF/py	ordered			
IMeBF/py^{a)}	0.654(3)	< 0.001	0.346(3)	< 0.001

^{a)} The molecule lies on a pseudo-twofold axis.

The change from **Br2BF/py** (ordered) to **BrMeBF/py** might have been expected to lead to an ordered arrangement. Given that one of the Br-atoms in the **Br2BF** complex does not interact with N or O, the Me could replace it with very little change in the packing. But there is disorder and it is such that both of the two major occupancies have the N₂O₂ end of the molecule in the same orientation. The disorder is primarily between Br and Me; that is, Me apparently has replaced Br on a nearly equal basis in interacting with the O-atoms. In contrast to the uncomplexed **BrMeBF**, there is a short CH₃⋯O distance. There is also a short ring H⋯O distance (*Table 4*). (See *Desiraju* and *Steiner* [7], for a discussion of C–H H-bonds).

When the change in the complex is from **BrMeBF** to **IMeBF**, the interaction changes from a Br⋯O to an I⋯N interaction, the only example of an X⋯N interaction in all the compounds described here. By contrast, in the series 5-halobenzofurazan 1-oxide (halo = Cl, Br, I) [8], there are Cl⋯N, Br⋯N, and I⋯O interactions. In this structure, there are two crystallographically independent **IMeBF** molecules. Both are involved in similar interactions, but one of the two shows significant disorder such that the I⋯N interaction is replaced by a CH₃⋯I interaction. The I⋯N contacts are at different distances but are geometrically similar. Again, as in the uncomplexed **IMeBF**, the CH₃⋯O distances are too long to be regarded as important contacts. There are also two short ring H⋯O distances that could be regarded as C–H H-bonds.

In these compounds, taken as a whole, the methyl group appears to be comparable in strength to Br as a *Lewis* acid or, at least, in its effect on the structures. On the other hand, in 5-methylbenzofurazan 1-oxide [9] there are no significant CH₃⋯O or CH₃⋯N interactions.

When this study was initiated, it was not expected to be this difficult to find ordered 5,6-disubstituted benzofurazan 1-oxides. In the structures of 4,7-dihalobenzofurazan 1-oxides (two polymorphs of the dichloro and one of the dibromoderivatives) there is no disorder in the N_2O_2 arrangement [9]; in these molecules, involving the same sorts of intermolecular interactions, the interactions are sufficient to order the molecules.

The formation of complexes did allow the unambiguous structures of the **Br2BF** and **IMeBF** molecules to be determined, something that could not be done in the disordered pure compounds. This is a possible route for the determination of other molecular structures that cannot be determined in the pure state owing to disorder or difficulty in preparing acceptable single crystals.

Crystallography: Experimental. – For all of the compounds given in *Table 2*, data were collected on a *Siemens SMART* area detector diffractometer [10], data reduction was done with SAINT [10], and solution and refinement were done with SHELXTL [11].

The sample of **Br2BF** was provided by Prof. *F. B. Mallory*. Crystals were grown from MeOH, EtOH, *i*-PrOH, benzene, acetone, $CHCl_3$, and CCl_4 . Fifteen crystals of varying morphology were examined, and all were isomorphous with the A polymorph of **Cl2BF**. The crystal used for the structure determination was grown from EtOH.

Crystals of **BrCIBF** were grown from the same solvents as mentioned above. Thirteen crystals of varying morphology were examined, and two polymorphs were found, isomorphous with the A and C polymorphs of **Cl2BF**. The crystal used for **BrCIBF-A** was a needle, and that used for **BrCIBF-C** was a prism, both grown from $CHCl_3$. A prism (C form) melted at 128° , while a needle (A form) turned opaque at $75-80^\circ$ and then melted at 128° . This suggests that the A form transformed to the C form at $75-80^\circ$, and that the C form is the stable one at high temperature.

The **BrMeBF** crystal used was a plate grown from CCl_4 . No search for polymorphs was made.

The **IMeBF** crystal used was a prism grown from acetone. No search for polymorphs was made.

The crystals used for all six complexes with pyrene were grown from acetone. No searches for polymorphs were made. The crystal used for **Br2PA/py** was twinned. The data were integrated with SAINTV6.35A [12] as a two-component nonmerohedral twin. TWINABS [13] found 15030 data from component 1, 15182 data from component 2, and 2721 including both components. R_{int} was 0.11 based on component 1. All systematic absences were removed with SYSABSFILTER [14]. All unpaired redundancies were removed with STRIP_REDUNDANT [14].

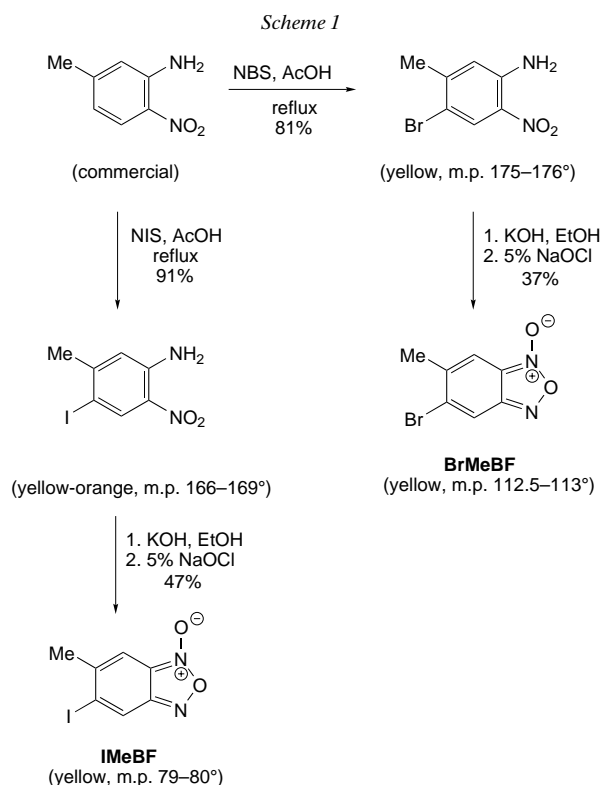
In almost every structure, disorder of the **BF** and **PA** molecules was present to some extent. Since the molecular dimensions could be estimated based on the earlier work, constraints could be used to help the refinement. In general, bond-length and angle restraints were introduced early in the refinement and then relaxed as far as possible without leading to an unstable refinement. The amount of relaxation possible varied from structure to structure and led to different numbers of restraints. In every case, overlapping atoms from the different orientations were constrained to have the same anisotropic displacement parameters. H-Atoms were included at idealized positions with isotropic displacement parameters 20% larger than the attached C-atoms for the

ring H and 50% larger for the Me H. No attempt was made to look for disorder in the Me groups.

The values of the occupancies of the various disordered species were determined by standard least-squares procedures [11]. The uncertainties quoted in *Table 5* are the standard uncertainties of least-squares refinement. Many of the parameters in the disordered structures are highly correlated, and, judging from the sensitivity of the occupancy parameters to small changes in other variables, the uncertainties should probably be twice as large. In spite of the uncertainties in the accuracies, the differences are clear as to the relative importance of the various occupancies in the disordered structures.

Synthesis: Discussion. – All three benzofurazan 1-oxides (**BrMeBF**, **IMeBF**, and **BrClBF**) were prepared conveniently by dropwise addition of aqueous 5% NaOCl to a red solution of the K salt of the corresponding 2-nitroaniline in ethanolic KOH. Disappearance of the red color of the anion indicates the end point, where the yellow color of the product remains in solution and in the precipitate. The NaOCl oxidation procedure (which probably goes through a nitrene intermediate) is essentially that of *Green and Rowe* [15] as used subsequently by us [9][16]. Two of the 2-nitroanilines were prepared (*Scheme 1*) by direct *para*-halogenation of 5-methyl-2-nitroaniline with *N*-bromosuccinimide (NBS) (giving 4-bromo-5-methyl-2-nitroaniline and then **BrMeBF**) or *N*-iodosuccinimide (NIS) (giving 4-iodo-5-methyl-2-nitroaniline and, then **IMeBF**) in refluxing glacial AcOH according to the procedure of *Gershon et al.* [17]. The third preparation proceeded (*Scheme 2*) through acetylation of 4-bromo-3-chloroaniline in aqueous solution [18] to give 4-bromo-3-chloroacetanilide, which was nitrated with KNO₃ in cold H₂SO₄ to the known 4-bromo-5-chloro-2-nitroacetanilide (previously prepared by *Wheeler and Valentine* [19] by nitration in cold fuming HNO₃ (*d* 1.52)). Our product appeared by its wide melting point and ¹H-NMR spectrum to be a mixture of isomers, possibly including the other product of *ortho*-nitration, 4-bromo-3-chloro-2-nitroacetanilide, which was removed by two crystallizations. Hydrolysis of the purified product in refluxing aqueous H₂SO₄ gave the known 4-bromo-5-chloro-2-nitroaniline (previously prepared by hydrolysis in boiling EtOH containing some conc. HCl [19]). This product was then subsequently oxidized with aqueous 5% NaOCl to **BrClBF**.

The complexes with pyrene were prepared by dissolving approximately equimolar amounts of both components in the solvent, with heating if necessary, and allowing evaporation of the solvent at room temperature. Initially, complexes were prepared of **Cl2BF** with hexamethylbenzene, pentamethylbenzene, 2,6-dimethylnaphthalene, pyrene, anthracene, phenanthrene, and triphenylene. Of these, the pyrene complex gave the best-quality crystals for diffraction experiments. Based on this, pyrene was used as the complexing agent for the remaining complexes.



Experimental Part

1. *General*. M.p.: uncorrected. NMR Spectra: *Varian Unity* 200- and 300-MHz spectrometers, chemical shifts in δ [ppm] downfield from TMS.

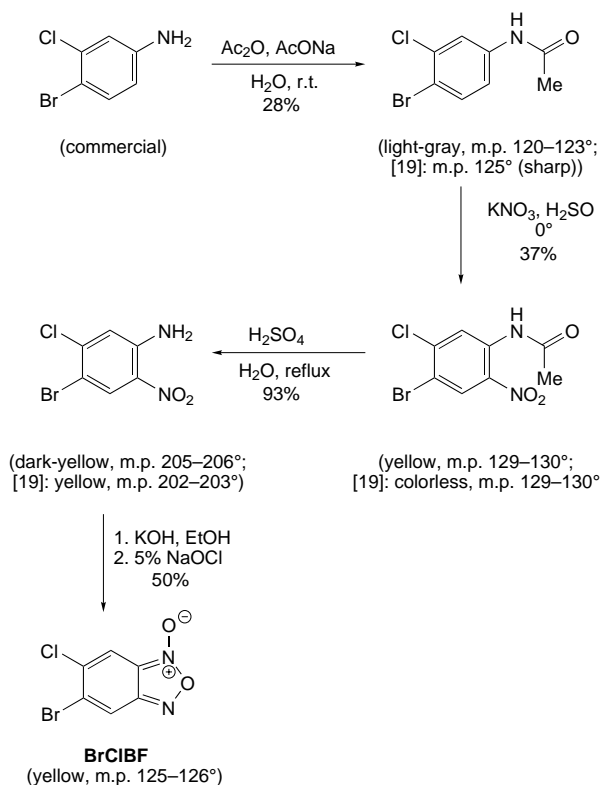
2. *4-Bromo-5-methyl-2-nitroaniline (Scheme 1)*: A soln. of 5-methyl-2-nitroaniline (1.00 g, 6.57 mmol) and *N*-bromosuccinimide (NBS; 1.15 g, 6.46 mmol) in glacial AcOH (100 ml) was refluxed, with stirring, for 80 min and then allowed to cool. The resulting mixture was poured into H₂O (900 ml), and the mixture was stirred for 10 min. The precipitate was suction-filtered and dried overnight to give a yellow solid (1.21 g, 5.24 mmol; 81%). M.p. 175–176°. ¹H-NMR ((D₆)DMSO): 8.05 (s, 1 H); 7.46 (s, 2 H); 6.94 (s, 1 H); 2.24 (s, 3 H).

3. *5-Bromo-6-methylbenzofurazan 1-Oxide (BrMeBF; Scheme 1)*. Ice-water-cooled aq. 5% NaOCl was added dropwise to a red, ice-cold soln. of 4-bromo-5-methyl-2-nitroaniline (76 mg, 0.329 mmol) in ethanolic KOH (35 ml). A precipitate formed but redissolved and, as addition continued, the soln. turned yellow, and a final precipitate formed. The mixture was extracted with CH₂Cl₂ (2 × 50 ml), and the extracts were dried (MgSO₄), filtered, and evaporated in a rotating evaporator, leaving a crude solid (76 mg). Recrystallization from EtOH gave **BrMeBF** as a yellow solid (28 mg, 0.122 mmol; 37%), M.p. 112.5–113°; ¹H-NMR (CDCl₃): 7.79 (s, 1 H); 7.30 (s, 1 H); 2.46 (s, 3 H).

4. *4-Iodo-5-methyl-2-nitroaniline (Scheme 1)*. A soln. of 5-methyl-2-nitroaniline (500 mg, 3.29 mmol) and *N*-iodosuccinimide (NIS; 665 mg, 2.96 mmol) in glacial AcOH (30 ml) was refluxed for 70 min and then allowed to cool for 5 min. The mixture was poured into ice-water (300 ml) and stirred for 10 min. The resulting precipitate was filtered, washed with cold H₂O (3 × 70 ml), and dried to give a yellow-orange solid (752 mg, 2.70 mmol; 91%). M.p. 166–169°. ¹H-NMR ((D₆)DMSO): 8.23 (s, 1 H); 7.42 (s, 2 H); 6.92 (s, 1 H); 2.24 (s, 3 H). ¹³C-NMR ((D₆)DMSO): 148.78; 146.28; 134.70; 130.11; 119.60; 82.83; 28.01.

5. *5-Iodo-6-methylbenzofurazan 1-Oxide (IMeBF; Scheme 1)*: Ice-water-cooled aq. 5% NaOCl was added dropwise to a red, ice-cold soln. of 4-iodo-5-methyl-2-nitroaniline (100 mg, 0.360 mmol) in ethanolic KOH

Scheme 2



(20 ml). A precipitate formed but redissolved and, as addition continued, the soln. turned yellow, and a final precipitate formed. This precipitate was extracted with CH_2Cl_2 (2×50 ml), and the combined org. extracts were dried (MgSO_4), filtered, and evaporated in a rotating evaporator, leaving a tan solid (84 mg). Crystallization from EtOH gave **IMeBF** (47 mg, 0.170 mmol; 47%). Yellow crystals. M.p. 79–80°. $^1\text{H-NMR}$ (CDCl_3): 8.11 (s, 1 H); 7.31 (s, 1 H); 2.49 (s, 3 H).

6. *4-Bromo-3-chloroacetanilide* (Scheme 2): The method of acetylation in aq. soln. was used [18]. 4-Bromo-3-chloroaniline (5.00 g, 24.2 mmol) and conc. HCl (1.99 ml, 24.2 mmol) in H_2O (100 ml) were stirred at r.t. for 20 min. Ac_2O (3.09 g, 30.3 mmol) and then anh. AcONa (3.29 g, 24.2 mmol) were added, producing a fluffy white precipitate. The mixture was stirred for 30 min, and the precipitate was filtered, washed with H_2O (100 ml), and dried to give a light tan solid (5.31 g, 21.4 mmol, 88%). Recrystallization from EtOH gave a light gray solid (1.70 g, 6.84 mmol; 28%). M.p. 120–123° ([19]: m.p. 125° (sharp)). $^1\text{H-NMR}$ ((D_6) acetone): 9.42 (s, 1 H); 8.06 (d, $J = 2.6$, 1 H); 7.61 (d, $J = 8.8$, 1 H); 7.42 (dd, $J = 8.8, 2.4$, 1 H); 2.02 (s, 3 H).

7. *4-Bromo-5-chloro-2-nitroacetanilide* (Scheme 2). This compound has been reported previously in 71% yield by nitration in cold fuming HNO_3 ($d = 1.52$) [19]. An ice-cold soln. of KNO_3 (230 mg, 2.02 mmol) in conc. H_2SO_4 (5 ml) was added, with stirring, to a soln. of 4-bromo-3-chloroacetanilide (500 mg, 2.02 mmol) in conc. H_2SO_4 (5 ml) at r.t. over a period of 2 min. The soln. turned brown and was stirred for 20 min and then poured onto ice (30 g). The resulting yellow precipitate was suction-filtered, washed with cold H_2O (80 ml), and dried on the filter for 30 min to give a yellow solid (530 mg, 1.84 mmol; 89%), which appeared from the wide m.p. and the $^1\text{H-NMR}$ spectrum to be a mixture of isomers (possibly including 4-bromo-3-chloro-2-nitroacetanilide). Two crystallizations from EtOH separated a single isomer as yellow crystals (270 mg, 0.92 mmol; 46%). M.p. 129–130° ([19] colorless, m.p. 129–130°). $^1\text{H-NMR}$ ((D_6) DMSO): 10.35 (s, 1 H); 8.32 (s, 1 H); 7.94 (s, 1 H); 2.07 (s, 3 H). $^{13}\text{C-NMR}$ ((D_6) DMSO): 169.28; 141.15; 138.85; 132.18; 130.11; 126.13; 116.56; 24.03.

8. *4-Bromo-5-chloro-2-nitroaniline* (Scheme 2). Preparation of this compound has been reported previously in unstated yield by hydrolysis of 4-bromo-5-chloro-2-nitroacetanilide with some conc. HCl in boiling EtOH [19]. A soln. of 4-bromo-5-chloro-2-nitroacetanilide (100 mg, 0.341 mmol) in H₂O (10 ml) and conc. H₂SO₄ (1.5 ml) was refluxed for 2.5 h, at which time TLC (silica gel; CH₂Cl₂) indicated that no starting material was present. The soln. was cooled, made alkaline to litmus with KOH pellets, and extracted with CH₂Cl₂. The extract was dried (MgSO₄) and evaporated in a rotating evaporator to leave a dark yellow solid (80 mg, 0.318 mmol; 93%). M.p. 205–206° ([19]; yellow, m.p. 202–203°). ¹H-NMR (CDCl₃): 8.38 (s, 1 H); 6.98 (s, 1 H); 6.08 (s, 2 H).

9. *5-Bromo-6-chlorobenzofurazan 1-Oxide* (**BrCIBF**; Scheme 2). Aq. 5% NaOCl was added dropwise to a red soln. of 4-bromo-5-chloro-2-nitroaniline (200 mg, 0.795 mmol) in ethanolic KOH (60 ml), and a yellow precipitate started to form, but addition was continued until precipitation stopped, and the solution turned yellow. The mixture was extracted with CH₂Cl₂ (3 × 100 ml), and the extracts were dried (MgSO₄), filtered, and evaporated in a rotating evaporator to leave a residue (180 mg) shown by TLC to contain a little starting material. Chromatography (silica gel; hexanes/CH₂Cl₂ 2:1) gave a better, but still slightly impure sample (160 mg). Crystallization from EtOH gave a yellow solid (100 mg, 0.401 mmol; 50%). M.p. 125–126°. ¹H-NMR (CDCl₃): 7.91 (s, 1 H); 7.68 (s, 1 H).

We thank Prof. *Frank B. Mallory* for the sample of **Br2BF**. We thank the *Wayland E. Noland Research Fellowship Fund* of the University of Minnesota Foundation for research support to *M. J. P.*

REFERENCES

- [1] C. R. Ojala, W. H. Ojala, D. Britton, J. Z. Gougoutas, *Acta Crystallogr., Sect. B* **1999**, 55, 530.
- [2] W. H. Ojala, 'Solid State Structures and Properties of Some Organic Strict Isosteres', Ph.D. Thesis, University of Minnesota, Minneapolis, MN, 1986.
- [3] D. S. Reddy, B. S. Goud, K. Panneerselvam, G. R. Desiraju, *Chem. Commun.* **1993**, 663.
- [4] D. Britton, *Acta Crystallogr., Sect. B* **2002**, 58, 553.
- [5] A. R. Katritzky, M. F. Gordeev, *Heterocycles* **1993**, 35, 483.
- [6] J. D. Dunitz, *Acta Crystallogr., Sect. B* **1995**, 51, 619.
- [7] G. R. Desiraju, T. Steiner, 'The Weak Hydrogen Bond', Oxford University Press, 1999.
- [8] M. Pink, D. Britton, *Acta Crystallogr., Sect. B* **2002**, 58, 116; R. C. Gehrz, D. Britton, *Acta Crystallogr., Sect. B* **1972**, 28, 1126.
- [9] D. Britton, W. E. Noland, *Acta Crystallogr., Sect. B* **1972**, 28, 1116.
- [10] Siemens, ASTRO and SAINT, Data Collection and Processing Software for the SMART System, *Siemens Analytical X-Ray Instruments, Inc.*, Madison, Wisconsin, USA, 1995.
- [11] G. M. Sheldrick, SHELXTL, Version 5.0. *Siemens Analytical X-Ray Instruments, Inc.*, Madison, Wisconsin, USA, 1994.
- [12] SAINTV6.35A, *Bruker AXS*, Madison, WI, 2002.
- [13] TWINABS v. 1.02, a) G. M. Sheldrick, 2002; b) R. Blessing, *Acta Crystallogr., Sect. A* **1995**, 51, 33.
- [14] SYSABSFILTER and STRIP_REDUNDANT, W. Brennessel, V. G. Young Jr., unpublished work, University of Minnesota, Minneapolis, MN, 2003.
- [15] A. G. Greene, F. M. Rowe, *J. Chem. Soc.* **1912**, 101, 2452; A. G. Greene, F. M. Rowe, *J. Chem. Soc.* **1913**, 103, 897, 2033; A. G. Greene, F. M. Rowe, *J. Chem. Soc.* **1917**, 111, 612.
- [16] D. Britton, W. E. Noland, *Chem. Ind. (London)* **1962**, 563; D. Britton, W. E. Noland, *J. Org. Chem.* **1962**, 27, 3218.
- [17] H. Gershon, D. D. Clarke, M. Gershon, *Monatsh. Chem.* **1994**, 125, 723.
- [18] L. F. Fieser, 'Experiments in Organic Chemistry', 3rd rev. edn., D. C. Heath and Co. Boston, 1957, p. 151–152.
- [19] H. L. Wheeler, W. Valentine, *Am. Chem. J.* **1899**, 22, 266.

Received January 27, 2003